Acta Scientific Applied Physics

Volume 2 Issue 8 August 2022

Review Article

Review on the Synthesis and the Application of Neutron Powder Diffraction in M-type Ferrites

Wang Shifa[1,2]*

[1]*School of Electronic and Information Engineering, Chongqing Three Gorges University, Chongqing Wanzhou, China*

[2]*Chongqing Key Laboratory of Geological Environment Monitoring and Disaster Early-warning in Three Gorges Reservoir Area, Chongqing Three Gorges University, Chongqing Wanzhou, China*

***Corresponding Author:** Wang Shifa, School of Electronic and Information Engineering, Chongqing Three Gorges University, Chongqing Wanzhou, China.

Received: July 13, 2022

Published: July 29, 2022

Abstract

Modern military industrial technology of radar anti-jamming ability and communication ability to put forward the new requirements, and M type ferrite in the airborne active phased array radar and the circulator used by 5G base station, and other fields has a great application prospect. By analyzing the magnetic structure of M-type ferrite, the important magnetic characteristic parameters of this type of magnetic material can be grasped, which provides experimental and theoretical basis for the design of new devices. In this paper, the crystal structure of M-type ferrite and the preparation methods of different forms of M-type ferrite are briefly introduced. The preparation of $BaFe_{12}O_{19}$ nanoparticles with special defect structure by gamma ray irradiation assisted polyacrylamide gel method is emphasized. The application of neutron powder diffraction in single phase M-type ferrite and element-doped M-type ferrite is reviewed. The magnetic structure of M-type ferrite is affected by different preparation methods, different doping elements, different doping ratio and different temperature of neutron powder diffraction spectrum. The analysis of magnetic structure of various M-type ferrites by neutron powder diffraction provides technical guarantee for the analysis of magnetic structure of multiple M-type ferrite complex, and further provides experimental basis for studying the internal correlation mechanism between magnetic properties and other physical and chemical properties.

Keywords: Radar Technology; 5G Base Station; M-type Ferrites; Neutron Powder Diffraction; Magnetic Structure

Introduction

The diversity of the formalization of modern war makes all countries rely more and more heavily on radar technology with high anti-interference ability and communication ability. The circulators used in airborne active phased array radar and 5G base station construction are inseparable from microwave ferrite [1,2]. However, when used in microwave devices, microwave ferrite does not need the bias provided by external permanent magnet, which is favored by researchers from all over the world. M-type ferrite is a kind of microwave ferrite, which has high remanence ratio, coercivity, saturation magnetization and high resistivity, and has been widely used in magnetic recording storage media, permanent magnets and other fields [3]. M-type ferrite has hexagonal crystal structure, and has been proved to have high thermal stability and chemical stability, high corrosion resistance, high microwave absorption properties, high near-infrared reflection, high anti-interference ability, high magnetic crystal anisotropy, high photocatalytic activity, high adsorption performance and high electrochemical properties. It has potential applications in microwave communication, next-generation battery systems, photocatalysts and adsorbents, etc. [4-7].

It is well known that the physical and chemical properties of M-type ferrite strongly depend on the preparation method. Excellent preparation methods can not only improve the physical and chemical properties of M-type ferrite itself, but also obtain some new properties, thus expanding its application range [3]. However, due to the limitation of its own characteristics, the physical and chemical properties of m-type ferrite in a single phase need to be achieved by the following two means in order to obtain novel properties and apply them in a broader field [8,9]: (1) Improve the physical and chemical properties of M-type ferrite by ion doping or element substitution; (2) Looking for other oxide semiconductor with excellent performance, combine it with M-type ferrite, so that it not only has the excellent performance of M-type ferrite, but also has the excellent performance of oxide semiconductor combined with it.

Compared with X-ray powder diffraction, neutron powder diffraction has unique advantages in resolving the crystal structure and magnetic structure of magnetic materials due to its strong neutron penetration ability, immunity from the influence of extranuclear electrons and magnetic moment [10]. The analysis of the crystal structure and magnetic structure of M-type ferrite and various magnetic materials with its main lattice is helpful to grasp the important characteristic parameters of this type of magnetic materials, and then provide experimental and theoretical support for the design and manufacture of related devices. In this paper, the crystal structure of M-type ferrites is briefly reviewed, and the methods of preparing pure M-type ferrites and the application of neutron scattering technology in the crystal structure and magnetic structure analysis of M-type ferrites and doped M-type ferrites are emphasized. The results provide technical reference for the subsequent application of neutron neutron powder diffraction in M-type ferrites, doped M-ferrites and multi-complex M-type ferrites.

Crystal structure of M-type ferrite

M-type ferrite is a kind of hexagonal ferrite (M, W, X, Y, Z, U), and its spontaneous magnetization is prefertively oriented to the C-axis. Its chemical formula was first proposed by Braun in Philips Laboratory in the late 1950s as $MFe_{12}O_{19}$ (M = Ba, Sr, Pb, Cu) [11]. As M-type ferrite has similar crystal structure, $BaFe_{12}O_{19}$ is taken as an example to describe its crystal structure.

Figure 1: Crystal structure of $BaFe_{12}O_{19}$ [3].

The space group of $BaFe_{12}O_{19}$ is P63/mmc, and the lattice constants a and c are 5.892 and 23.183 Å, respectively. Figure 1 shows the crystal structure of $BaFe_{12}O_{19}$. The unit cell is composed of two S blocks $(Fe_6O_8)^{2+}$ without Ba^{2+} and R blocks $(BaFe_6O_{11})^{2+}$ with Ba^{2+} oxygen ion layer. The S block consists of four octahedrons and two tetrahedrons, while the R block consists of one hexahedron and five tetrahedrons. The 24 Fe^{3+} ions in the unit cell, 16 spin up and 8 spin down are located at three octahedral sites (2a, 12k and $4f_2$), one tetrahedral site ($4f_1$) and one triangular bipyramidal site (2b), respectively.

Preparation method of M-type ferrite

M-type ferrites with different morphologies, shapes and sizes have different physical and chemical properties. Therefore, researchers often adopt different preparation methods to synthesize M-type ferrites with different morphologies, shapes and sizes according to special requirements. M-type ferrite mainly exists in the form of single crystal, thin film, block material and powder. The preparation of block material is mainly based on high temperature and high pressure, solid phase sintering, which requires high equipment. At present, the preparation methods of single crystal for the M-type ferrite mainly include floating zone method [12], flux method [13], molten salt method [14], etc. The synthesis of single crystal is beneficial to observe the magnetic domain structure of M-type ferrite. The preparation of thin films for

the M-type ferrite mainly includes DC magnetron sputtering [15], pulse laser deposition [16], chemical vapor deposition [17], sol-gel method [18], etc. M-type ferrite films prepared have been widely used in magnetic memory, radio frequency equipment, microwave devices and other fields. To preparation the M type ferrite single crystal, thin film and bulk material, need technical means or device and synthesis conditions of the demand is higher, and M type ferrite powder especially nanometer powder, without high-end equipment and could be regulated and controlled by process parameters for synthesis of M type ferrite nano powder of different particle size, the nano powder tend to show a more excellent than the piece of wood or novel physical and chemical properties. Therefore, there are many researches on the preparation of M-type ferrite nano-powders.

Figure 2: Flow chart of $BaFe_{12}O_{19}$ nanoparticles prepared by a gamma ray irradiation assisted polyacrylamide gel method, in which the cobalt source is used by the Cobalt source irradiation facility of Institute of Nuclear Physics and Chemistry.

In recent years, the synthesis methods of M-type ferrite nano-powders mainly include sol-gel method, hydrothermal method, coprecipitation method, high-energy ball milling method, self-combustion method, ammonium nitrate melting method, polyacrylamide gel method and so on [3,19,20]. Among these methods, polyacrylamide gel method is an effective method to synthesize highly dispersed magnetic metal oxide nanoparticles. The method mainly using chelating agents such as citric acid, ethylenediamine tetraacetic acid, tartaric acid, etc will be precursor solution of complexation metal ions to form complex, again with acrylamide and methylene double acrylamide polymerization of polyacrylamide network limit metal complex in the network and forming gel, gel drying and sintering process so as to obtain the ultimate target products. There are usually three polymerization initiation modes of acrylamide and methylene bisacrylamide: (1) polymerization initiator initiation; (2) thermal polymerization initiation; (3) ray polymerization initiation. The ray polymerization initiation mode has uniform energy and is easy to synthesize nano powders with uniform particles. No odor is produced in the synthesis process, which greatly reduces the environmental pollution. The synthesized nanoparticles have special defect structure, which improves the physical and chemical properties of the target product. The author and his research group [21] first proposed that the polymerization of $MgFe_2O_4$ precursor was initiated by gamma ray irradiation polymerization in the cobalt source irradiation facility of Institute of Nuclear Physics and Chemistry, Chinese Academy of Engineering Physics, and highly dispersed $MgFe_2O_4$ nanoparticles were prepared. At the same time, the crystal structure of $MgFe_2O_4$ was analyzed by the neutron powder diffraction spectrum of Mianyang Research Reactor. The results show that the $MgFe_2O_4$ nanoparticles have a special defective structure, which overcomes the defect of high recombination rate of electronic and hole in the bulk $MgFe_2O_4$ and has excellent photocatalytic activity. Subsequently, the synthesis of highly dispersed metal oxide nanoparticles by gamma ray irradiation polymerization has attracted extensive attention of researchers, and luminescent materials, photocatalysts, adsorbents and magnetic materials have been synthesized by this method. In 2021 year, our research group [3] used this method to synthesize M-type ferrite nano-powder ($BaFe_{12}O_{19}$) with high magnetic moment ratio, and its preparation process is shown in figure 2.

Application of neutron powder diffraction in M-type ferrite

M-type ferrites have strong magnetic properties and have unique advantages in the characterization of their crystal structure and magnetic structure by neutron powder diffraction. The coercivity, remanence and saturation magnetization of m-type ferrite can be improved by ion doping or other oxides doping, and the anisotropy field can be reduced. By measuring the neutron powder diffraction spectrum of these m-type ferrites, the magnetic structure of these m-type ferrites can be observed, and the experimental basis for explaining their magnetic mechanism can be provided. In recent years, because $MFe_{12}O_{19}$ (M = Ba, Sr) ferrite in M-type ferrite is easy to synthesize and has high magnetic properties, researchers

have analyzed the crystal structure and magnetic structure of pure phase $MFe_{12}O_{19}$ (M = Ba, Sr) ferrite by synthesizing single crystal or powder. Meanwhile, In, Ga, Al, Sc and various multielement doped $MFe_{12}O_{19}$ (M = Ba, Sr) were characterized by neutron powder diffraction. Interestingly, Sc doping in $BaFe_{12}O_{19}$ and $SrFe_{12}O_{19}$ produces a longitudinal conical magnetic order, whose cone angle around the c axis increases with the increase of Sc concentration. These doped M-type ferrite compounds exhibit type II polyferroicity in a transverse magnetic field with a ferroelectric polarizability of about 25 μ cm^{-2} [22]. It is of great significance to characterize these significant results and analyze their magnetic structures by neutron powder diffraction.

Application in pure phase $MFe_{12}O_{19}$ (M = Ba, Sr)

Figure 3: Magnetic structure of $BaFe_{12}O_{19}$: (a) Collinear magnetic structure; (b) Coordination polyhedra of Fe^{3+} ion; (c) Longitudinal conical magnetic structure. [22].

As early as in 1950s, Gorter., *et al*. [23] systematically studied the crystal structure and magnetic structure of $BaFe_{12}O_{19}$, and theoretically calculated its saturation magnetization of 20 μB. According to Gorter model, M-type $BaFe_{12}O_{19}$ has colinear magnetic sequence arranged along the C-axis, as shown in Figure 3(a). Figure 3(b) shows three coordination polyhedra of Fe^{3+} ion in $BaFe_{12}O_{19}$. Figure 3(c) shows the longitudinal conical magnetic structure of $BaFe_{12}O_{19}$. Cao., *et al*. [24] refined the magnetic structure of $BaFe_{12}O_{19}$ single crystal based on this linear model. Collomb., *et al*. [25] prepared polycrystalline $BaFe_{12}O_{19}$ using $BaCO_3$ and Fe_2O_3 as raw materials by high temperature solid state reaction method, and analyzed the crystal structure and magnetic structure of $BaFe_{12}O_{19}$ by neutron powder diffraction. The magnetic moments of Fe1 (2a), Fe2 (2b), Fe3 ($4f_1$), Fe4 ($4f_2$) and Fe5 (12k) are 4.1, 4.8, -4.5, -4.2 and 4.9 mB, respectively. A similar result was obtained by testing $BaFe_{12}O_{19}$ on neutron powder diffraction spectrometer in Mianyang Research Reactor, except that gamma ray irradiation assisted polyacrylamide gel method was used to synthesize $BaFe_{12}O_{19}$ nanoparticles [3]. The spectrogram is shown in figure 4. For the $SrFe_{12}O_{19}$, there are few literatures on the characterization of its crystal structure and magnetic structure by neutron powder diffraction, and only Heineck., *et al*. [26] prepared the corresponding powder material by mechanical ball milling and characterized its crystal structure.

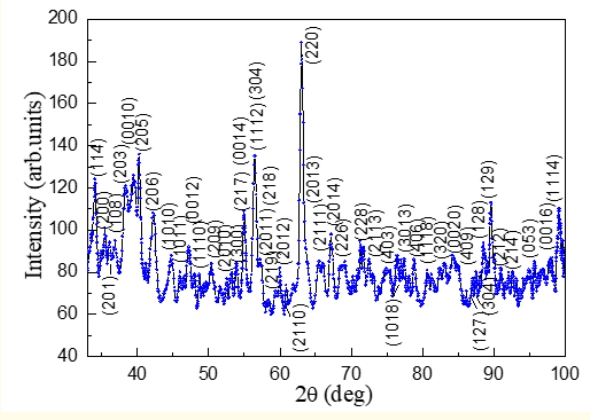

Figure 4: Neutron powder diffraction spectrum of $BaFe_{12}O_{19}$ measured by Mianyang Research Reactor [3].

Application in MFe_{12}-xInxO_{19} (M = Ba, Sr)

Figure 5: Magnetic structure of $BaFe_{12-x}In_xO_{19}$ (x = 2): (a) Ferrimagnetic structure model; (b) longitudinal conical magnetic structure; (c) schematic of conical magnetic structure making an angle 29.33° with c-axis; (d) Spin structure as viewed along c-axis [36].

When different elements replace parts of Fe, they may exhibit different magnetic behaviors than m-type ferrites. Albanese., *et al*. [27] studied In-doped $BaFe_{12}O_{19}$ using magnetization and Musbauer spectrum data, and found that its magnetic order was nonlinear in nature at low temperature. However, Trukhanov., *et al*. [28-30] came to the opposite conclusion based on neutron diffraction measurement data, believing that the magnetic structure of In-doped $BaFe_{12}O_{19}$ is collinear. Recently, Turchenko., *et al*. [31] also reported the multi-iron properties of $BaFe_{12-x}In_xO_{19}$ (x = 0.1-1.2), which induced spontaneous polarization by an applied electric field. It is also concluded that the magnetic structure is collinear within the concentration range of In doping studied. Similarly, the magnetic structure observed in In-doped $SrFe_{12}O_{19}$ is colinear [32]. However, recent reports suggest that the local electric dipole may be caused by the shift of iron outside the equatorial plane at the position of the triangular bipyramid [33]. Wang., *et al*. [34] attributed the observation of antiferroelectric defeat to the existence of such a local dipole moment and proposed the possibility of the existence of magnetic quantum quasi-electric states from the measurement of magnetic specific heat. Gupta., *et al*. [35] found through neutron powder diffraction measurements that magnetic Fe^{3+} was partially replaced by non-magnetic indium, and the magnetic moment value at the corresponding position decreased, resulting in a decrease in the total magnetic moment. In addition, with the doping of indium ions at the iron site, the exchange between the magnetic sulattices weakens and the magnetic moment value decreases. The total magnetic moment of In-doped $BaFe_{12}O^{19}$ is 7.25 μB. $BaFe_{10}In_2O_{19}$ shows complex magnetic behavior below 110 K, with coexistence of long-range conical magnetic sequence and cluster spin glass magnetic sequence [36]. The magnetic structure of the corresponding neutron powder diffraction spectrum is shown in figure 5.

Application in $BaFe_{12-x}(Ga, Al)_xO_{19}$

In complex magnetic oxides, the hybridization of the electron shell layer is very complex and therefore requires finer neutron diffraction data than the X-ray powder diffraction spectrum. Trukhanov., *et al*. [37] prepared $BAFe_{12-x}Ga_xO_{19}$ ferrite by traditional solid state reaction method, and compared the effects of XRD data and neutron powder diffraction data on $BaFe_{12-x}Ga_xO19$ ferrite cell parameters and cell volume. At temperature (T), the total magnetic moment of each unit cell can be calculated according to Formula (1):

$$M_{total}(T) = [m_{2a}(T)] + [m_{2b}(T)] - 2[[m_{4f_{IV}}(T) + m_{4fVI}(T)]] + 6[m_{12k}(T)] \quad \text{----- (1)}$$

If the magnetic moment of Fe^{3+} at 0 K is 5 μB, the magnetic moment of $BaFe_{12}O_{19}$ per unit cell is 20 μB. Due to the increase of thermal vibration of ions forming lattice, the disorder of magnetic moment in space is caused. The total magnetic moment of $BaFe_{12-x}Ga_xO_{19}$ ferrite gradually decreases with the increase of doping amount x. For the same reason, similar phenomena have been observed in $BaFe_{12-x}Al_xO_{19}$ ferrite synthesized by the solid phase reaction method [38]. Figure 6 shows the magnetic structure of $BaFe_{12-x}Al_xO_{19}$ analyzed according to Gorter model [39]. The magnetic moments of Fe^{3+} atoms are all along the direction of the easy magnetization axis, which coincides with the c axis [40,41]. Since the distribution of Al ions is largely affected by the method of sample preparation, further studies are needed to confirm the distribution of Al ions at the corresponding crystal locations.

Figure 6: Magnetic structure of $BaFe_{12-x}Al_xO_{19}$ on the basis of Gorter model: Fe^{3+} ion has magnetic moment, Ba^{2+} ion has no magnetic moment [39].

Application in $BaFe_{12-x}Sc_xO_{19}$

In early studies, researchers believed that the magnetic structure changed from colinear to conical in the temperature range of 10-77 K after the non-magnetic scandium (Sc) ion partially replaced the Position of Fe^{3+} [42]. Tokunaga., *et al*. [43] observed from single crystal neutron diffraction measurements that the conical helical magnetic structure of $BaFe_{12-x-\delta}Sc_xMg_\delta O_{19}$($\delta$ = 0.05) single crystal was located at 370 K when Sc concentration x = 1.75. Due to the change of magnetic structure from longitudinal cone to transverse cone, they also observed ferroelectric behavior induced by magnetic field. However, previous studies only focused on longitudinal conical magnetic transitions observed in the 200-300 K range and did not consider magnetization behavior at low temperatures. Therefore, Gupta., *et al*. [44] reported direct evidence of spin-like glass behavior in $BaFe_{12-x}Sc_xO_{19}$ systems below 50 K. Evidence for the co-existence of such spinal-like glass behavior and long-range conical magnetic structures has been found from neutron diffraction studies. The magnetic structure of $BaFe_{12-x}Sc_xO_{19}$ is shown in figure 7. In the doped (Sc) sample, although the structure is still ferromagnetic, the spin arrangement of iron ions does not follow the Gorter model. In this case, the Fe magnetic moments at sites 2a, $4f_1$, $4f_2$ and 12k are parallel along the positive direction of the c-axis, while the Fe magnetic moments at site 2b are parallel along the negative direction of the c-axis, and therefore antiparallel to other sites [45]. Krezhov., *et al*. [46] prepared $BaFe_{10.4}Sc_{1.6}O_{19}$ by softening method. Combining neutron diffraction, field-dependent ^{57}Fe Mossbauer spectroscopy and magnetic measurement, the collinear block structure was still effective at 300 K and below to about 190 K. In the 190-1.6 K range, a complex block-shaped conical structure was observed that was not proportional to temperature. $Ba(Fe_{1-x}Sc_x)_{12}O_{19}$ ferrite prepared by ceramic technology has a non-collinear structure at x > 0.05 by neutron powder diffraction characterization [47]. Darwish., *et al*. [48] prepared $BaFe_{12-x}Sc_xO_{19}$ ferrite using the same preparation method, and observed non-collinear magnetic order above x>0.6.

Application in $MFe_{12}O_{19}$(M = Ba, Sr)

Single element doping is difficult to meet the growing market demand and the device performance requirements are different, it is necessary to use multi-element substitution to obtain special magnetic performance parameters. As early as the end of last century, the neutron powder diffraction experiment of multi-element substitution of $BaFe_{12}O_{19}$ has been carried out. Wartewig., *et al*. [49] prepared polycrystalline $BaFe_{12-2x}Zn_xTi_xO_{19}$(x = 0, 0.4, 0.8, 1.2, 1.6, 2.0) ferrite by acetic acid solution decomposition. By comparing the magnetic structure of neutron powder diffraction spectrum with the magnetic data measured by superconducting quantum interferometer, The magnetic data obtained by the two are basically consistent. Kreisel., *et al*. [50] found through neutron powder diffraction spectrum characterization analysis that the special change in magnetic anisotropy of $BaFe_{12-2x}Ir_xCo_xO_{19}$ single crystal was related to the substitution of Fe^{3+} ions at the 4e bipyramidal site by Ir^{4+}. Krezhov., *et al*. [51] prepared $BaFe_{10.3}Co_{0.85}Ti_{0.85}O_{19}$ microcrystalline and nanocrystalline by softening method, and determined its crystal structure by neutron powder diffraction spectrum, laying a foundation for the subsequent study of magnetic structure. Mudsainiyan., *et al*. [52] prepared $BaCo_xZr_xFe_{(12-2x)}O_{19}$ ferrite by sol-gel method. Neutron powder diffraction analysis found that, The magnetization and magnetocrystal anisotropy of $BaCo_xZr_xFe_{(12-2x)}O_{19}$ ferrite are related to the distribution of Co-Zr ion at five Fe^{3+} sites. With the increase of the types of element doping, the factors affecting the magnetic properties of each component are also increasing. Therefore, it is increasingly difficult to analyze the magnetic structure of

Figure 7: Magnetic structure of $BaFe_{12-x}Sc_xO_{19}$. Fe1: red, Fe2: blue, Fe3: green, Fe4: yellow and Fe5: orange. [45].

such magnetic ferrites by neutron powder diffraction spectrum. Comparatively, the application of neutron powder diffraction in M-type ferrites with multi-element doping is less than that of single element doping.

Conclusion and Prospect

The special physical and chemical properties of M-type ferrite make it have important applications in defense industry, 5G base station construction, magnetic recording media, microwave devices, photocatalysts and adsorbents and other fields. Due to its high magnetic properties, neutron powder diffraction has unique advantages in characterizing the magnetic structure of magnetic materials. It is superior to XRD in crystal structure analysis and consistent with the magnetic data measured by superconducting quantum interferometer. Therefore, this technology has become the preferred equipment for characterizing magnetic materials. Combined with the crystal structure of M-type ferrite, the preparation methods of m-type ferrite with different morphology were summarized in this paper, and the application of gamma ray irradiation assisted polyacrylamide gel method in the synthesis of M-type ferrite was emphasized. The application of neutron powder diffraction in magnetic structure analysis of single phase of M-type ferrite and element-doped M-type ferrite is reviewed.

With the increase of doping elements, each component has a great influence on the magnetic properties, and it is difficult to explore the magnetic structure of the multi-component doped ferrite. The neutron powder diffraction characterization of M-type ferrites with multi-element doping is obviously less than that of M-type ferrites with single element doping. In addition, the neutron powder diffraction study of M-type ferrite is still in the exploratory stage. Recently, carbon quantum dots (CQDs)/CeO_2/$MFe_{12}O_{19}$ magnetic separation photocatalysts with double heterojunctions have been proved to have high photocatalytic activity and adsorption properties. It is of great significance to obtain the neutron powder diffraction spectrum of the photocatalysts and analyze their magnetic structure to study the effect of magnetic components on the photocatalytic activity of the photocatalysts. Meanwhile, insight into the internal correlation mechanism between magnetic properties and photocatalytic activity can provide the corresponding experimental basis for in-depth study of the photocatalytic mechanism and adsorption mechanism of the magnetic separation photocatalyst.

Competing Interests

The authors declare that they have no competing interests.

Acknowledgments

This work was supported by the NSAF joint Foundation of China (U2030116), the Science and Technology Research Program of Chongqing Education Commission of China (KJZD-K202001202), the Chongqing Key Laboratory of Geological Environment Monitoring and Disaster Early-warning in Three Gorges Reservoir Area (No. ZD2020A0401), the Talent Introduction Project (09924601) of Chongqing Three Gorges University.

Bibliography

1. Chen Yuying. "Application prospect of microwave ferrite material in 5G communication base station". *The Journal of New Industrialization* 10.3 (2020): 106-110.

2. Zhai Zongmin and Jiang Yunshi. "Ferrite phase shifter successive flux feedback phase compensation technology". *Journal of Magnetic Materials and Devices* 49.4 (2018): 55-57+76.

3. Wang S F., *et al*. "M-type barium hexaferrite nanoparticles synthesized by γ-ray irradiation assisted polyacrylamide gel method and its optical, magnetic and supercapacitive performances". *Journal of Cluster Science* 32 (2021): 569-578.

4. Xu X and Song W. "A new application field for $BaFe_{12}O_{19}$ used as visible light photocatalyst". *Materials Technology* 35.7 (2020): 395-401.

5. Polley K., *et al*. "Adsorption and sunlight-induced photocatalytic degradation of methyl blue by $BaFe_{12}O_{19}$ ferrite particles synthesised through co-precipitation method". *International Journal of Environmental Analytical Chemistry* (2021): 1-20.

6. Wang S F., *et al*. "A comparative study on the phase structure, optical and NIR reflectivity of $BaFe_{12}O_{19}$ nano-pigments by the traditional and modified polyacrylamide gel method". *Journal of Nano Research* 67 (2021): 1-14.

7. Wang S F., *et al*. "Synthesis of novel CQDs/CeO_2/$SrFe_{12}O_{19}$ magnetic separation photocatalysts and synergic adsorption-photocatalytic degradation effect for methylene blue dye removal". *Chemical Engineering Journal Advances* 6 (2021): 100089.

8. Gupta S., *et al*. "Effect of scandium substitution on magnetic and transport properties of the M-type barium hexaferrites". *Journal of Alloys and Compounds* 815 (2020): 152467.

9. Xie M., *et al*. "Preparation of magnetically recoverable and Z-scheme $BaFe_{12}O_{19}$/AgBr composite for degradation of 2-Mercaptobenzothiazole and Methyl orange under visible light". *Applied Surface Science* 521 (2020): 146343.

10. Guo Erjia and Zhu Tao. "Application of neutron scattering in magnetic materials research". *Physics* 48.11 (2019): 708-714.

11. Braun P B. "The crystal structures of a new group of ferromagnetic compounds". *Philips Research Report* 12 (1957): 491-548.

12. Dho J., *et al*. "Effects of the grain boundary on the coercivity of barium ferrite $BaFe_{12}O_{19}$". *Journal of Magnetism and Magnetic Materials* 285.1-2 (2005): 164-168.

13. Fisher J G., *et al*. "Growth of single crystals of $BaFe_{12}O_{19}$ by solid state crystal growth". *Journal of Magnetism and Magnetic Materials* 416 (2016): 384-390.

14. Arendt R H. "The molten salt synthesis of single magnetic domain $BaFe_{12}O_{19}$ and $SrFe_{12}O_{19}$ crystals". *Journal of Solid State Chemistry* 8.4 (1973): 339-347.

15. Zhang X., *et al*. "$BaFe_{12}O_{19}$ films prepared on Al_2O_3 (0 0 0 1) by direct current magnetron sputtering". *Materials Letters* 248 (2019): 24-27.

16. Carosella C A., *et al*. "Pulsed laser deposition of epitaxial $BaFe_{12}O_{19}$ thin films". *Journal of Applied Physics* 71.10 (1992): 5107-5110.

17. Pignard S., *et al*. "Epitaxial and polycrystalline $BaFe_{12}O_{19}$ thin films grown by chemical vapour deposition". *Thin Solid Films* 350.1-2 (1999): 119-123.

18. Santos J V A., *et al*. "$BaFe_{12}O_{19}$ thin film grown by an aqueous sol–gel process". *Microelectronics Journal* 34.5-8 (2003): 565-567.

19. Liang Q., *et al*. "Structural, magnetic and microwave properties of $Ba_{1-x}Nd_xFe_{12}O_{19}$". *Journal of Magnetism and Magnetic Materials* 539 (2021): 168400.

20. Yensano R and Phokha S. "Effect of pH on single phase $BaFe_{12}O_{19}$ nanoparticles and their improved magnetic properties". *Journal of Materials Science: Materials in Electronics* 31.14 (2020): 11764-11773.

21. Wang S., *et al*. "A novel method for the synthesize of nanostructured $MgFe_2O_4$ photocatalysts". *Journal of Sol-Gel Science and Technology* 84.1 (2017): 169-179.

22. Kumar K., *et al*. "Evidence for conical magnetic structure in M-type $BaFe_{12}O_{19}$ hexaferrite: A combined single-crystal X-ray magnetic circular dichroism and neutron diffraction study". *Physica Status Solidi (RRL)–Rapid Research Letters* 15.6 (2021): 2000506.

23. Gorter E W. "Saturation magnetization of some ferrimagnetic oxides with hexagonal crystal structures". *Proceedings of the IEE-Part B: Radio and Electronic Engineering* 104.5 (1957): 255-260.

24. Cao H B., *et al*. "High pressure floating zone growth and structural properties of ferrimagnetic quantum paraelectric $BaFe_{12}O_{19}$". *Applied Materials* 3.6 (2015): 062512.

25. Collomb A., *et al*. "Neutron diffraction studies of some hexagonal ferrites: $BaFe_{12}O_{19}$, $BaMg_2$-W and $BaCo_2$-W". *Journal of Magnetism and Magnetic Materials* 62.1 (1986): 57-67.

26. Heinecke U., *et al*. "Structural transformations and connected changes of magnetic properties by mechanical treatment of $SrFe_{12}O_{19}$". *Physica Status Solidi A* 77.1 (1983): 225-232.

27. Albanese G and Deriu A. "Magnetic properties of Al, Ga, Sc, in substituted barium ferrites: A comparative analysis". *Ceramurgia International* 5 (1979): 3-10.

28. Trukhanov S V., *et al*. "Temperature evolution of the structure parameters and exchange interactions in $BaFe_{12-x}In_xO_{19}$". *Journal of Magnetism and Magnetic Materials* 466 (2018): 393-405.

29. Trukhanov., *et al*. "Polarization origin and iron positions in indium doped barium hexaferrites". *Ceramics International* 44.1 (2018): 290-300.

30. Trukhanov A V., *et al*. "Critical influence of different diamagnetic ions on electromagnetic properties of $BaFe_{12}O_{19}$". *Ceramics Internatio*nal 44.12 (2018): 13520-13529.

31. Turchenko V A., *et al*. "Features of crystal structure and dual ferroic properties of $BaFe_{12-x}Me_xO_{19}$ (Me=In^{3+} and Ga^{3+}; x= 0.1-1.2)". *Journal of Magnetism and Magnetic Materials* 464 (2018): 139-147.

32. Turchenko V A., *et al*. "Magnetic and ferroelectric properties, crystal and magnetic structures of $SrFe_{11.9}In_{0.1}O_{19}$". *Physica Scripta* 95.4 (2020): 044006.

33. Rensen J G and Van Wieringen J S. "Anisotropic Mossbauer fraction and crystal structure of $BaFe_{12}O_{19}$". *Solid State Communications* 7 (1969): 1139-1141.

34. Wang P S and Xiang H J. "Room-temperature ferrimagnet with frustrated antiferroelectricity: Promising candidate toward multiple-state memory". *Physical Review X* 4 (2014): 011035.

35. Gupta S., *et al*. "Spin-phonon coupling mediated magneto-dielectricity in indium doped barium hexaferrite ($BaFe_{10.5}In_{1.5}O_{19}$)". *Journal of Magnetism and Magnetic Materials* 492 (2019): 165717.

36. Gupta S., *et al*. "Magnetodielectricity induced by coexisting incommensurate conical magnetic structure and cluster glass-like states in polycrystalline $BaFe_{10}In_2O_{19}$". *Journal of Alloys and Compounds* 825 (2020): 154141.

37. Trukhanov A V., *et al*. "Features of crystal and magnetic structure of the $BaFe_{12-x}Ga_xO_{19}$ (x≤2) in the wide temperature range". *Journal of Alloys and Compounds* 791 (2019): 522-529.

38. Trukhanov A V., *et al*. "Evolution of structure and magnetic properties for $BaFe_{11.9}Al_{0.1}O_{19}$ hexaferrite in a wide temperature range". *Journal of Magnetism and Magnetic Materials* 426 (2017): 487-496.

39. Trukhanov A V., *et al*. "Crystal structure and magnetic properties of the $BaFe_{12-x}Al_xO_{19}$ (x= 0.1–1.2) solid solutions". *Journal of Magnetism and Magnetic Materials* 393 (2015): 253-259.

40. Trukhanov A V., *et al*. "Features of crystal structure and magnetic properties of M-type Ba-hexaferrites with diamagnetic substitution". *International Journal of Materials Chemistry and Physics* 1.3 (2015): 286-294.

41. Trukhanov A., *et al*. "Evolution of structure and physical properties in Al-substituted Ba-hexaferrites". *Chinese Physics B* 25.1 (2015): 016102.

42. Aleshko-Ozhevskii O P., *et al*. "A neutron diffraction study of the structure of magnetoplumbite". *Soviet Physics Crystallography* 14.3 (1969): 367-369.

43. Tokunaga Y., *et al*. "Multiferroic-type hexaferrites with a room-temperature conical state and magnetically controllable spin helicity". *Physical Review Letters* 105 (2010): 257201.

44. Gupta S., *et al*. "Observation of magnetoelastic and magnetoelectric coupling in Sc doped $BaFe_{12}O_{19}$ due to spin-glass-like phase". *Journal of Physics: Condensed Matter* 31.29 (2019): 295701.

45. Gupta S., *et al*. "Effect of scandium substitution on magnetic and transport properties of the M-type barium hexaferrites". *Journal of Alloys and Compounds* 815 (2020): 152467.

46. Krezhov K. "Effects of Substitution in Barium Hexaferrites $BaFe_{12-x}X_xO_{19}$ (X= Co, Ti, Sc)". *Solid State Phenomena* 159 (2010): 175-180.

47. Trukhanov A V., *et al*. "Pecularities of the magnetic structure and microwave properties in Ba $(Fe_{1-x}Sc_x)_{12}O_{19}$ (x<0.1) hexaferrites". *Journal of Alloys and Compounds* 822 (2020): 153575.

48. Darwish M A., *et al*. "Tuning the magnetic order in Sc-substituted barium hexaferrites". *IEEE Magnetics Letters* 10 (2019): 1-5.

49. Wartewig P., *et al*. "Magnetic properties of Zn-and Ti-substituted barium hexaferrite". *Journal of Magnetism and Magnetic Materials* 192.1 (1999): 83-99.

50. Kreisel J., *et al*. "The magnetic anisotropy change of $BaFe_{12-2x}Ir_xCo_xO_{19}$: A single-crystal neutron diffraction study of the accompanying atomic and magnetic structures". *Journal of Magnetism and Magnetic Materials* 213.3 (2000): 262-270.

51. Krezhov K., *et al*. "Neutron powder diffraction study of (Co, Ti)-substituted fine-particle Ba-hexaferrite". *Applied Physics A* 74.1 (2002): s1086-s1088.

52. Mudsainiyan R K., *et al*. "Cations distribution and magnetic properties of Co–Zr doped $BaCo_xZr_xFe_{(12-2x)}O_{19}$ prepared via citrate precursor sol–gel route". *Ceramics International* 40.10 (2014): 16617-16626.